

<https://helda.helsinki.fi>

---

## Rapid and Direct Preparation of Lignin Nanoparticles from Alkaline Pulping Liquor by Mild Ultrasonication

Agustin, Melissa

2019-12-16

---

Agustin , M , Penttilä , P , Lahtinen , M & Mikkonen , K S 2019 , ' Rapid and Direct Preparation of Lignin Nanoparticles from Alkaline Pulping Liquor by Mild Ultrasonication ' , ACS Sustainable Chemistry & Engineering , vol. 7 , no. 24 , pp. 19925-19934 . <https://doi.org/10.1021/acssuschemeng.9b05445>

---

<http://hdl.handle.net/10138/321466>

<https://doi.org/10.1021/acssuschemeng.9b05445>

---

unspecified

acceptedVersion

---

*Downloaded from Helda, University of Helsinki institutional repository.*

*This is an electronic reprint of the original article.*

*This reprint may differ from the original in pagination and typographic detail.*

*Please cite the original version.*

Article

## Rapid and direct preparation of lignin nanoparticles from alkaline pulping liquor by mild ultrasonication

Melissa B. Agustin, Paavo A. Penttilä, Maarit Lahtinen, and Kirsi S. Mikkonen

*ACS Sustainable Chem. Eng.*, **Just Accepted Manuscript** • DOI: 10.1021/acssuschemeng.9b05445 • Publication Date (Web): 13 Nov 2019

Downloaded from pubs.acs.org on November 20, 2019

### Just Accepted

“Just Accepted” manuscripts have been peer-reviewed and accepted for publication. They are posted online prior to technical editing, formatting for publication and author proofing. The American Chemical Society provides “Just Accepted” as a service to the research community to expedite the dissemination of scientific material as soon as possible after acceptance. “Just Accepted” manuscripts appear in full in PDF format accompanied by an HTML abstract. “Just Accepted” manuscripts have been fully peer reviewed, but should not be considered the official version of record. They are citable by the Digital Object Identifier (DOI®). “Just Accepted” is an optional service offered to authors. Therefore, the “Just Accepted” Web site may not include all articles that will be published in the journal. After a manuscript is technically edited and formatted, it will be removed from the “Just Accepted” Web site and published as an ASAP article. Note that technical editing may introduce minor changes to the manuscript text and/or graphics which could affect content, and all legal disclaimers and ethical guidelines that apply to the journal pertain. ACS cannot be held responsible for errors or consequences arising from the use of information contained in these “Just Accepted” manuscripts.

1  
2  
3  
4  
5  
6  
7  
8 1 Rapid and direct preparation of lignin  
9  
10  
11  
12  
13  
14 2 nanoparticles from alkaline pulping liquor by  
15  
16  
17  
18  
19  
20 3 mild ultrasonication  
21  
22  
23  
24  
25  
26

27 4 *Melissa B. Agustin<sup>†\*</sup>, Paavo A. Penttilä<sup>‡</sup>, Maarit Lahtinen<sup>†</sup>, Kirsi S. Mikkonen<sup>†,§\*</sup>*  
28  
29  
30

31  
32 5 <sup>†</sup>Department of Food and Nutrition, P.O. Box 66 (Agnes Sjöbergin katu 2), FI-00014  
33  
34

35 6 University of Helsinki, Finland  
36  
37  
38

39  
40 7 <sup>‡</sup> Department of Bioproducts and Biosystems, P.O. Box 16300, FI-00076 Aalto  
41  
42

43 8 University, Finland  
44  
45  
46

47  
48 9 <sup>§</sup>Helsinki Institute of Sustainability Science (HELSUS), P.O. Box 65, FI-00014 University  
49  
50  
51 10 of Helsinki, Finland  
52  
53  
54

55  
56 11 \*Corresponding authors:  
57  
58  
59  
60

12 Email: [kirsi.s.mikkonen@helsinki.fi](mailto:kirsi.s.mikkonen@helsinki.fi)

13 Email: [melissa.agustin@helsinki.fi](mailto:melissa.agustin@helsinki.fi)

14

15 KEYWORDS: Lignin nanoparticle, ultrasonication, acid precipitation, alkaline pulping

16 liquor, emulsion, BLN lignin

17 ABSTRACT. The production of lignin nanoparticles (LNPs) has opened new routes to

18 utilization of lignin in advanced applications. The existing challenge, however, is to

19 develop a production method that can easily be adapted on an industrial scale. In this

20 study, we demonstrated a green and rapid method of preparing LNPs directly from a

21 sulfur-free alkaline pulping liquor by combining acid-precipitation and ultrasonication. The

22 combined method produced spherical LNPs, with hierarchical nanostructure and highly

23 negative surface charge, within only 5-min of sonication. The mild, rapid sonication was

24 achieved by sonicating directly without prior drying the acid-precipitated and dialyzed

25 lignin. Optimization of the method revealed the potential for minimizing acid consumption,

26 shortening the dialysis time, and processing directly the alkaline liquor with as much as

20 wt% lignin. The isolated LNPs were stable during storage for 180 days, at a pH range of 4–7 and in a dispersing medium below 0.1 M NaCl. The LNPs also displayed excellent emulsifying properties, stabilizing oil-in-water emulsions. Thus, this simple and energy-efficient method opens a sustainable, straightforward and scalable route to production of solvent-free LNPs, with high potential as interface stabilizers of multi-phase systems in the food and medical industries.

## INTRODUCTION

Lignin, with its highly irregular polyphenolic structure, is the most abundant natural aromatic polymer on Earth.<sup>1</sup> Representing 15–40% of the dry weight of lignocellulosics,<sup>2</sup> lignin is one of the major by-products in the pulp and paper industries, with an estimated global production of 50 million tons per year.<sup>3,4</sup> Lignin production is expected to continuously increase as the demand for second-generation biofuel, i.e. biofuels from nonfood sources, is realized. In the USA alone, the mandate to produce 79 billion liters of second-generation biofuels by 2022 translates into the production of 62 million tons of

lignin, with the assumption that the sourced biomass constitutes about 28% lignin and a biofuel yield of 355 L ton<sup>-1</sup> of dry biomass.<sup>5</sup> In addition, the emerging green technologies in utilizing bio-based materials, especially cellulose from wood, signal that more lignin is yet to be produced when such technologies are adapted on an industrial scale. Despite wide availability, lignin is still considered as an undervalued material, since most of it is only burned for energy recovery in the pulping process.<sup>2</sup> This limitation has been attributed to the heterogeneous structure and properties of lignin, which vary with the source and method of isolation.<sup>6</sup> However, lignin's complex structure provides it with unique properties, including antimicrobial, antioxidant, UV-blocking, and emulsifying properties.<sup>6,7</sup> These unique properties, coupled with attributes typical for bio-based materials, such as being renewable, sustainable, biodegradable, and abundant, make lignin a promising material for advanced and sophisticated applications.

Exhaustive efforts in recent years have resulted in development of technologies that provide high-value applications for use of lignin. Some notable applications, which are summarized in various reviews,<sup>6–10</sup> include using lignin as binders, adsorbents, precursors for carbon-fiber production, adhesives, emulsifiers, or as engineering

materials in the development of smart composites. Recently, the conversion of lignin into nanoscale particles has become increasingly recognized. The formation of LNPs enables lignin, which is typically insoluble in water, to form a colloidal dispersion in aqueous systems,<sup>7</sup> which is attractive from the industrial point of view. The formation of nanostructured lignin also allows better control of morphology and structure, enabling the produced LNPs to blend well in various host matrices.<sup>10</sup> LNPs, similar to other materials in nanoscale form, exhibit chemical and physical interactions, mainly governed by their surface properties.<sup>11</sup>

Several methods for preparing LNPs from various types of lignin have been reported but only few attempts were made for large scale LNP production.<sup>12,13</sup> The feasibility for scaling up was hindered because most of the current laboratory-scale methods are energy-intensive, consume considerable number of reagents, and produce only a very dilute LNP suspension.<sup>12</sup> Thus, a method that can easily be scaled up to industrial level is still an ongoing quest.

Among the various methods of LNP preparation, acid precipitation, solvent-shifting, and disintegration by mechanical treatment have become increasingly favored. Acid

precipitation, which was first reported by Frangville et al.,<sup>14</sup> involves the gradual addition of an acid to a solution of lignin in aqueous alkali or in ethylene glycol<sup>15</sup>. Solvent-shifting involves dissolving lignin in an organic solvent such as tetrahydrofuran (THF),<sup>16–18</sup> dimethyl-sulfoxide (DMSO),<sup>19</sup> and dioxane<sup>20</sup>. It is then followed by the gradual introduction of an antisolvent, which is often water, enabling the self-assembly of LNPs.<sup>16</sup> Mechanical treatment, such as high-shear homogenization<sup>21,22</sup> or ultrasonication,<sup>23–25</sup> applies force to disintegrate to nanoscale level the lignin usually dispersed in water.

Ultrasonication, when used as a method for LNP preparation, offers the advantage of simplicity and eliminates the use of toxic organic solvents. In this method, ultrasound waves (20 kHz to 10 MHz) are applied to a medium, causing the formation of microscopic bubbles that generate heat and pressure when they collapse during the process called cavitation.<sup>26</sup> The generated pressure is powerful enough to disintegrate lignin particles to nanoscale level; however, very low initial lignin concentrations (< 1 wt%) and at least 1 h of sonication were used in previous reports.<sup>23–25</sup> Long sonication times can result in extensive oxidation, producing radicals that can initiate radical-induced polymerization. Phenolic hydroxyl (OH) groups in lignin can form phenoxy radicals during sonication and



1  
2  
3  
4 90 may induce crosslinking reactions.<sup>27</sup> Thus, to avoid radical-induced polymerization,  
5  
6  
7 91 shortening the sonication time is necessary. This could be reached without necessarily  
8  
9  
10 92 increasing the intensity of the applied ultrasound waves by changing the properties of the  
11  
12  
13  
14 93 starting lignin material. In contrast to previous reports in which the starting lignin material  
15  
16  
17 94 was dried before sonication, here we used a never-dried lignin material produced directly  
18  
19  
20  
21 95 from alkaline pulping liquor (APL) by acid precipitation. Our hypothesis is that drying  
22  
23  
24 96 greatly changes the surface properties of the lignin, inducing agglomeration and making  
25  
26  
27  
28 97 lignin recalcitrant to mechanical disintegration. We propose here a high-yield method to  
29  
30  
31 98 recover and subsequently disintegrate to nanoparticles the lignin dissolved in APL. This  
32  
33  
34  
35 99 method is a combination of two conventional LNP preparation methods: acid-precipitation  
36  
37  
38 100 and ultrasonication. The mild ultrasonication is achieved by directly disintegrating without  
39  
40  
41  
42 101 prior drying the acid-precipitated lignin, thereby making the overall process energy  
43  
44  
45 102 efficient, rapid, straightforward, and highly scalable. Thus, this solvent-free method,  
46  
47  
48  
49 103 coupled with the utilization of a sulfur-free BLN (from the initials of the inventor's names)  
50  
51  
52 104 pulping liquor, which was used for the first time in LNP preparation, paved the way toward  
53  
54  
55  
56  
57  
58  
59  
60

production of green odor-free LNPs that exhibited excellent emulsifying properties when used as stabilizers of oil-in-water emulsions.

## EXPERIMENTAL SECTION

### Materials

The APL, with approximately 20 wt% lignin from birch (*Betula* L.), was provided by CH-Bioforce Oy (Espoo, Finland). It is a sulfur-free pulping liquor produced through a novel biomass fractionation method known as the BLN process,<sup>28</sup> which enables the isolation of lignin of high purity. A detailed chemical characterization of the acid-precipitated lignin obtained from this APL is available elsewhere.<sup>29</sup> Reagent-grade hydrochloric acid (HCl), nitric acid (HNO<sub>3</sub>), and sulfuric acid (H<sub>2</sub>SO<sub>4</sub>) were purchased from Merck (Darmstadt, Germany). The nuclear magnetic resonance (NMR) solvent d<sub>6</sub>-DMSO was purchased from Eurisotop (Saint-Aubin, France). Rapeseed oil (Keiju, Bunge Finland Ltd, Raisio, Finland) for emulsion preparation was purchased from a local supermarket.

### Lignin nanoparticle preparation

1  
2  
3  
4 121 The LNPs were prepared by a combined acid precipitation and mild ultrasonication  
5  
6  
7 122 method. In all, 100 g of 3.5 wt% lignin solution, which was prepared from the APL by  
8  
9  
10 123 dilution in deionized water, was stirred vigorously, followed by rapid addition of 100 mL of  
11  
12  
13  
14 124 0.25 M acid (HCl, HNO<sub>3</sub>, or H<sub>2</sub>SO<sub>4</sub>). The resulting mixture, which had a pH of about 2,  
15  
16  
17 125 was centrifuged for 7 min at 8000 rpm to remove most of the salts and acids, and the  
18  
19  
20  
21 126 residue was collected and diluted with water to maintain the initial concentration. The  
22  
23  
24 127 mixture was then dialyzed against 5 L of distilled water, using Spectra/Por 1 (6–8 kDa  
25  
26  
27  
28 128 molecular-weight cutoff) for 3 days, replacing the water at least six times. The final pH of  
29  
30  
31 129 the suspension only reached about 4 after dialysis. The dialyzed mixture (80 g) was kept  
32  
33  
34  
35 130 in an ice bath, sonicated using a Branson digital sonicator at a frequency of 20 kHz and  
36  
37  
38 131 80% oscillation amplitude (100 W). A 5-mL sample was collected after 2 min, and the  
39  
40  
41  
42 132 sonication was continued for a total of 5 min.

#### 43 44 45 133 46 47 134 Hydrodynamic diameter and $\zeta$ -potential measurement

48  
49  
50  
51 135 The hydrodynamic diameter ( $D_H$ ) and  $\zeta$ -potential of the isolated LNPs were determined  
52  
53  
54  
55 136 by the dynamic light scattering (DLS) technique using a Zetasizer Nano-ZS Zen 3600

(Malvern Instruments Ltd., Worcestershire, UK) equipped with a laser (4 mW, 632.8 nm) and backscatter detection at 173° to eliminate the effect of multiple scattering. The optimum concentration was determined by serial dilution of a stock solution containing 40 mg mL<sup>-1</sup> LNPs. The dilutions showed no significant differences and a concentration of 4 mg mL<sup>-1</sup> was chosen in the following measurements. At least three measurements with 12–15 runs per measurement were performed for each sample. For the ζ-potential, a folded capillary cell at 25 °C and an applied electric field of 40 V were used. LNP suspensions (4 mg mL<sup>-1</sup>) with a pH of about 5 were prepared by dilution with deionized water. The electrophoretic mobility data obtained from the measurement were converted to the ζ-potential using the Smoluchowski model. At least five measurements involving 10–15 runs per measurement were performed for each sample. All data were processed using the built-in DTS software (DTS Software, LLC.; Raleigh, NC, USA)

Chemical structure characterization

1  
2  
3  
4 151 The chemical structure of the acid-precipitated lignin before and after sonication was  
5  
6  
7 152 characterized by acquiring the Fourier-transform infrared (FTIR) spectra and the two-  
8  
9  
10 153 dimensional (2D) heteronuclear single-quantum coherence (HSQC) 2D NMR spectra.

11  
12  
13  
14 154 The FTIR spectra were recorded using a SpectrumOne (PerkinElmer, Turku, Finland),  
15  
16  
17 155 equipped with a universal attenuated total reflectance accessory. A background scan was  
18  
19  
20  
21 156 performed before the sample, which was scanned 16 times at a resolution of 4 cm<sup>-1</sup>. The  
22  
23  
24 157 spectra were recorded between 4000 and 600 cm<sup>-1</sup> and the baseline corrected using the  
25  
26  
27  
28 158 built-in software.

29  
30  
31 159 For the NMR analysis, performed at 27 °C, the samples (20 mg) were dissolved in d<sub>6</sub>-  
32  
33  
34  
35 160 DMSO (0.7 mL). The spectra were acquired using a Bruker Avance 850 MHz III high-  
36  
37  
38 161 definition spectrometer equipped with a cryoprobe (Bruker Corp., MA, USA). The  
39  
40  
41  
42 162 experiments were performed using the pulse program hsqcedetgpsisp.2, and the  
43  
44  
45 163 following parameters: size of the FID 2048, pulse width 7.8 μs, number of dummy scans  
46  
47  
48  
49 164 32, and number of scans 16. The spectral widths used were 12 ppm in the <sup>1</sup>H dimension  
50  
51  
52 165 and 220 ppm in the <sup>13</sup>C dimension.  
53  
54  
55

56 166  
57  
58  
59  
60

## 167 Atomic force microscopy

168 The morphology of the synthesized LNPs was characterized using the Veeco  
169 Multimode V (Veeco Instruments Inc., Santa Barbara, CA, USA) atomic force microscope  
170 (AFM). The sample was prepared by dropping a dilute aqueous suspension of LNPs onto  
171 a freshly cleaved mica plate and drying in air. The imaging was performed under ambient  
172 conditions using Si probes (Bruker Corp., CA, USA) with a nominal tip radius of 8 nm, a  
173 nominal spring constant of 3 N m<sup>-1</sup>, and a resonant frequency of 75 kHz. The images were  
174 recorded in tapping mode, and basic image plane leveling was applied to remove artifacts  
175 caused by sample tilt.

## 177 Small-angle x-ray scattering

178 Small-angle x-ray scattering (SAXS) experiments were carried out on beamline B21 at  
179 the Diamond Light Source, equipped with a high-throughput, small-volume liquid-handling  
180 robot (BioSAXS; Arinax Scientific Instrumentation, MAATEL SAS, Moirans, France) and  
181 an Eiger detector (Dectris AG, Baden-Daettwil, Switzerland). The x-ray wavelength was  
182 0.947 Å and the sample-to-detector distance 2.7 m. A 50-μL volume of HCl-precipitated

183 LNP with approximate concentrations of 1 mg mL<sup>-1</sup> and 10 mg mL<sup>-1</sup> in water were injected  
 184 in a glass capillary, and the SAXS data were collected as a series of 20 frames with 2-s  
 185 exposure times while the sample flowed through the capillary. The initial data reduction,  
 186 including transmission correction, azimuthal integration, and scaling to absolute intensity  
 187 against a water sample, was performed automatically with Data Analysis Workbench  
 188 (DAWN) software (<http://dawnsi.org/>), while SAXSutilities software  
 189 (<http://www.saxsutilities.eu/>) was used for subsequent frame averaging, water-  
 190 background subtraction, and rebinning.

191 The SAXS intensities were fitted with the unified exponential/power-law model,<sup>30</sup> with  
 192 two levels of structural hierarchy ( $N = 2$ ):

$$193 \quad I(q) = \sum_{i=1}^N G_i e^{\left(-\frac{q^2 R_{g,i}^2}{3}\right)} + B_i e^{\left(-\frac{q^2 R_{g,(i+1)}^2}{3}\right)} \left(\frac{[erf(q R_{g,i}/\sqrt{6})]^3}{q}\right)^{P_i} + C \quad (1)$$

194 In the model of Eq. 1, each level of structural hierarchy contributes to the scattering in  
 195 the form of a Guinier function (term with coefficient  $G_i$ ) at low  $q$  and a power law (term  
 196 with coefficient  $P_i$ ) at high  $q$ . The radius of gyration  $R_{g,i}$  describes the dimensions of the  
 197 structural elements of level  $i$  and corresponds to radius  $R = \sqrt{5/3} R_{g,i}$  in the case of a solid

sphere. The power-law exponent  $P_i$  describes the aggregation state of subunits with radius of gyration  $R_{g(i)}$ , with higher values of  $P_i$  indicating denser packing. A manually adjusted constant background ( $C$ ) was included in the fits when necessary. Fitting was done using the Differential Evolution Adaptive Metropolis (DREAM) algorithm in SasView 4.2 software,<sup>31</sup> and the reported error estimates for the fitting parameters were based on those given by the software.

#### Stability test

The stability of the LNPs was assessed by monitoring the changes in  $D_H$  and  $\zeta$ -potential during storage, and with variation in the pH and ionic strength of the dispersing medium. For the storage test, stock LNP suspensions (40 mg mL<sup>-1</sup>) were kept in a cold room for 6 months. A small volume of the sample was drawn from the stock solution at each time interval and diluted 10-fold for the analysis of  $D_H$ . The stability of the HCl-precipitated LNP against variation in pH and ionic strength of the dispersing medium was tested by determining the  $D_H$  of the LNP dispersed in solutions with differing pH or ionic strength.



213 Solutions with various pH were prepared by adjusting the pH with aqueous HCl or NaOH.

214 Aqueous NaCl solutions (0.1 M –1M) were used to vary the ionic strength.

215

216 Optimization

217 The method was optimized by monitoring the  $D_H$  and  $\zeta$ -potential while varying the

218 concentration of the acid, the initial concentration of lignin in the suspension, and

219 precipitation pH. For the variation in acid concentration and initial lignin concentration, the

220 same procedure as in the preparation with different acids was used. The only difference

221 was that the volume of acid solution needed to precipitate the lignin to pH 2 varied when

222 different concentrations of acids were used or when the initial lignin concentration was

223 varied. To determine the optimum pH for precipitation, sequential pH precipitation was

224 performed. A lignin solution (7 wt%, 200 g) prepared from the APL was fractionated

225 sequentially at pH 6, 4, and 2 by adding 0.25 M HCl. All the residues obtained from the

226 various pH values were redispersed in deionized water, dialyzed for 2 days, and then

227 sonicated to produce LNPs. A known weight of the LNP suspension was also freeze-dried

228 to determine the fractional yield at each pH.

229

230

231 Emulsion preparation and characterization

232 Four formulations of oil-in-water emulsion with 10 wt% rapeseed oil and varying

233 amounts of LNPs (0.15, 0.30, 0.45, and 0.60 wt%) were prepared. A coarse emulsion

234 was initially prepared by mixing for 2 min at 22,000 rpm the mixture (oil, water and LNPs)

235 using an UltraTurrax (T-18 basic; IKA, Staufen, Germany). The coarse emulsion was then

236 passed four times through a high-pressure homogenizer (Microfluidizer 110Y;

237 Microfluidics, Westwood, MA, USA) at a pressure of 88 bar to obtain finer droplet size.

238 The morphology of the emulsion droplets was characterized using an optical

239 microscope (AxioScope A1; Carl Zeiss Inc., Oberkochen, Germany) equipped with a built-

240 in camera, within 1 h after the preparation. The stability of the emulsion was monitored

241 using a Turbiscan LAB stability analyzer (Formulaction SA, Toulouse, France), equipped

242 with an optical reading head that scans the entire height of the sample at 40- $\mu$ m intervals.

243 All measurements were done at 25 °C by scanning three times a turbiscan vial containing

20-mL of emulsion. The first measurement was performed within 1 day of the preparation, and succeeding measurements were done once per day.

## RESULTS AND DISCUSSION

### Effect of acid type

The type of acid can influence the final properties of the lignin recovered from APL by acid precipitation<sup>21</sup>. Regardless of the type of acid, the size distribution of all LNPs was monodisperse, yielding a single peak in the size distribution chromatogram and had an averaged polydispersity index of 0.20 (Figure 1a). HCl and HNO<sub>3</sub> produced LNPs with an average  $D_H$  of about 96 nm after only 2 min of sonication (Figure 1b). The average  $D_H$  further decreased to about 80 nm when the sonication time was increased to 5 min. H<sub>2</sub>SO<sub>4</sub> showed slightly higher  $D_H$  than HCl and HNO<sub>3</sub>, but still yielded nanoparticles with less than 100-nm diameter after 5 min of sonication. The process also afforded high yield, enabling a final LNP suspension with more than 3 wt% lignin. The percentage yield of LNPs, calculated from the amount of LNPs recovered after freeze-drying with respect to

the initial amount of lignin in the solution before precipitation, ranged from 86% to 93%, with HCl giving the highest yield.

Varying the types of acid resulted in similar values of the  $\zeta$ -potential of the lignin before sonication and of the subsequent LNPs after sonication (Figure 1c). The average  $\zeta$ -potential of the isolated LNPs was about -63 mV and was similar to that of LNPs synthesized from softwood kraft lignin by solvent-shifting method.<sup>16</sup> The highly negative surface charge of lignin has been attributed to abundant phenolic groups and to adsorbed OH groups, typical for hydrophobic molecules in contact with water.<sup>14,16</sup> This highly negative surface charge contributes to the stabilization of particles in colloidal suspension by creating sufficient electric double-layer repulsion. The  $\zeta$ -potential values, however, became more negative after ultrasonic treatment. This finding suggests that ultrasonication can induce changes in the surface charge of lignin, possibly by exposing to the surface carboxyl or phenolic groups that were initially inside of the lignin aggregates. The increase in the absolute  $\zeta$ -potential stabilized the resulting LNP suspension, which did not exhibit particle sedimentation similar to the unsonicated lignin suspension during storage.

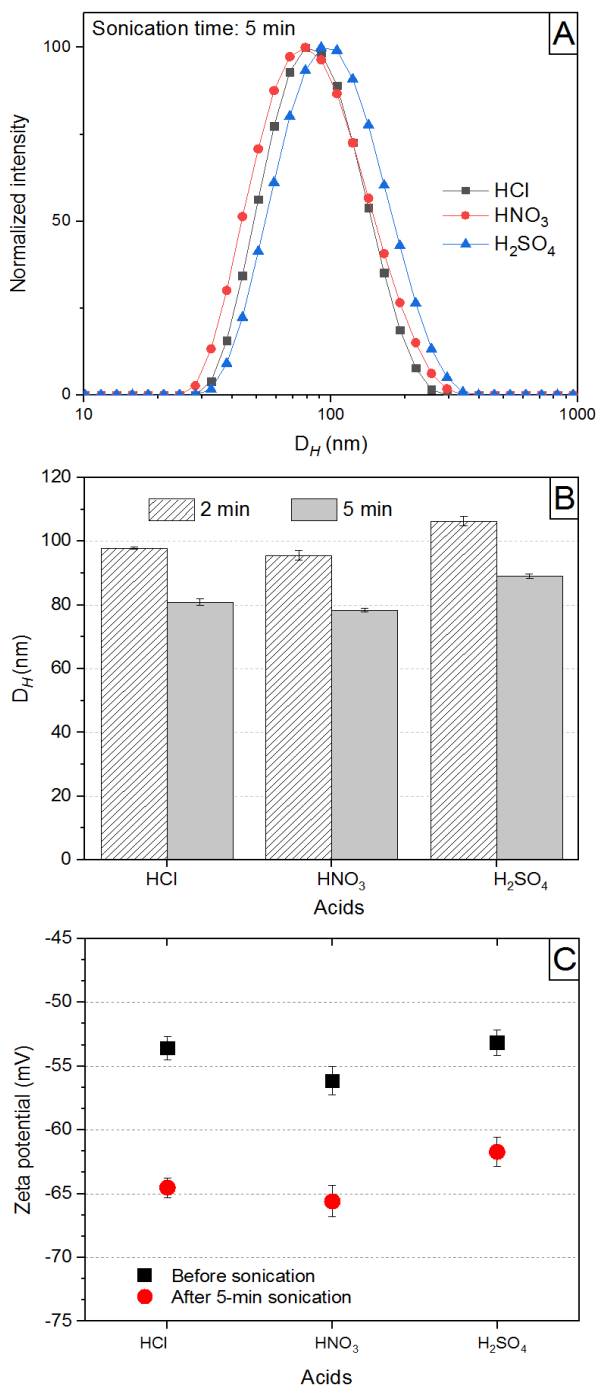


**Figure 1.** Effect of acid type on the intensity-based hydrodynamic diameter ( $D_H$ ) distribution (a), average  $D_H$  (b), and average zeta potential (c) of lignin nanoparticles prepared from alkaline pulping liquor by the combined acid precipitation and

ultrasonication method. The error bars represent  $\pm$  standard deviations of at least three measurements.

## Characterization

The isolated LNPs were further characterized for their chemical characteristics, morphology in the dry state, and nanostructure in aqueous systems. All the results presented in Figure 2 pertain to the LNPs produced by HCl precipitation at pH 2 and with 5-min sonication time. The results for the LNPs isolated from  $\text{HNO}_3$  and  $\text{H}_2\text{SO}_4$  precipitation, when available, are provided in the supplementary information.

The chemical characteristics of the acid-precipitated lignin and the subsequent LNPs produced from them were investigated using FTIR and 2D HSQC NMR.

All FTIR spectra (Figures 2a and S1) showed absorption bands typical for lignin (Table S1). No significant changes, such as increase in intensities or shifting of absorption peak to different frequencies, were observed after ultrasonication. The phenolic and aliphatic hydroxyl groups gave the broad absorption band from  $3100\text{--}3600\text{ cm}^{-1}$ . The sharpening of this absorption band towards high frequency was not observed, which is in contrast to

the findings of Garcia-Gonzalez et al<sup>24</sup>. According to them, ultrasonication induced partial oxidation to lignin resulting in an increase in OH groups that form intramolecular hydrogen bonds. The 5-min we used compared to the 6-h sonication time used by Garcia-Gonzalez et al<sup>24</sup> is possibly mild enough not to cause oxidations. A sharp signal at 1640 cm<sup>-1</sup> attributed to carbonyl stretching vibrations of intramolecularly hydrogen-bonded carboxylic acids<sup>24</sup> was also not detected, which further confirmed that the mild ultrasonication did not cause oxidation. The strong peak at 1109 cm<sup>-1</sup>, which can be due to C–O deformation in methoxyl groups, did not show significant decrease in intensity after ultrasonication. Yin et al<sup>25</sup> applied 1-h sonication to a slightly alkaline suspension of lignin and reported a decrease in the absorption intensity at 1105 cm<sup>-1</sup> due to potential cleavage of C–O bonds. Overall, the FTIR spectra revealed no significant change in the structure of the lignin before and after mild ultrasonication.

The unchanged chemical structure was further confirmed using 2D HSQC NMR analysis of acid-precipitated lignin and LNPs. The spectra of both samples were identical confirming the result of FTIR analysis, which showed that mild ultrasonication did not induce chemical modifications of lignin. Furthermore, the obtained HSQC spectra were

1  
2  
3  
4 310 nearly identical compared to the previously published HSQC spectrum of BLN lignin <sup>29</sup>.  
5  
6

7 311 The 2D HSQC NMR spectrum of LNPs is provided in Figure S2.  
8  
9

10 312 The morphology of the isolated LNPs in the dry state (Figures 2b and S3) was  
11  
12  
13  
14 313 investigated using AFM. Due to agglomeration during drying, it was not possible to  
15  
16  
17 314 measure individually the dimensions of the particles. Nevertheless, the results clearly  
18  
19  
20  
21 315 showed that the isolated LNPs were generally spherical, with lateral and vertical  
22  
23  
24 316 dimensions not exceeding 100 nm.  
25  
26

27  
28 317 SAXS was used to determine the outer dimensions and inner structure of the LNPs in  
29  
30  
31 318 aqueous suspension at two different concentrations (1 mg mL<sup>-1</sup> and 10 mg mL<sup>-1</sup>). The  
32  
33  
34  
35 319 SAXS intensities of the samples (Figure 2c) showed clear indications of structural  
36  
37  
38 320 hierarchy, with shoulder features located slightly below  $q = 0.01 \text{ \AA}^{-1}$  and approx.  $q = 0.05$   
39  
40  
41 321  $\text{\AA}^{-1}$ , and power-law scattering in between. The intensities were therefore fitted with the  
42  
43  
44  
45 322 unified exponential/power-law model of Eq. 1 (solid lines in Figure 2c, different  
46  
47  
48  
49 323 contributions of the terms shown in Figure S4), which yields information on the  
50  
51  
52 324 dimensions and packing density at each level of structural hierarchy in mass fractal  
53  
54  
55  
56 325 aggregates.<sup>30</sup>  
57  
58  
59  
60



Based on the fitting results (Table S2), the samples consisted of mass fractal aggregates of smaller subunits. The radius of gyration of the aggregates or clusters, as determined from the intensity around the first shoulder (level  $i = 1$ ), was 23–27 nm ( $R_{g,1}$  in Table S2). Under the assumption of spherical particles, this would translate into a diameter of about 60–70 nm, which is in excellent agreement with the hydrodynamic radius determined with DLS (~80 nm). The power-law exponent of level  $i = 1$  ( $P_1$  in Table S2) was approx. 2.5, indicating that the space inside of the aggregates was not fully filled with solid material. This is in contrast to previous SAXS results for dry lignin<sup>32</sup> and LNPs in water,<sup>33</sup> which showed power-law exponents close to 4 arising from compact particles with smooth surfaces. The dimensions of the subunits forming the aggregates in the current samples was deduced from the second shoulder feature of the SAXS intensities ( $i = 2$ ), yielding a radius of gyration between 4.2 nm and 5.0 nm ( $R_{g,2}$  in Table S2) and sphere diameter of 11–13 nm. The power-law exponent of this level ( $P_2$  in Table S2) probably describes the inner structure of the clustering subunits, and its values were in line with rather compact particles or collapsed polymer chains.

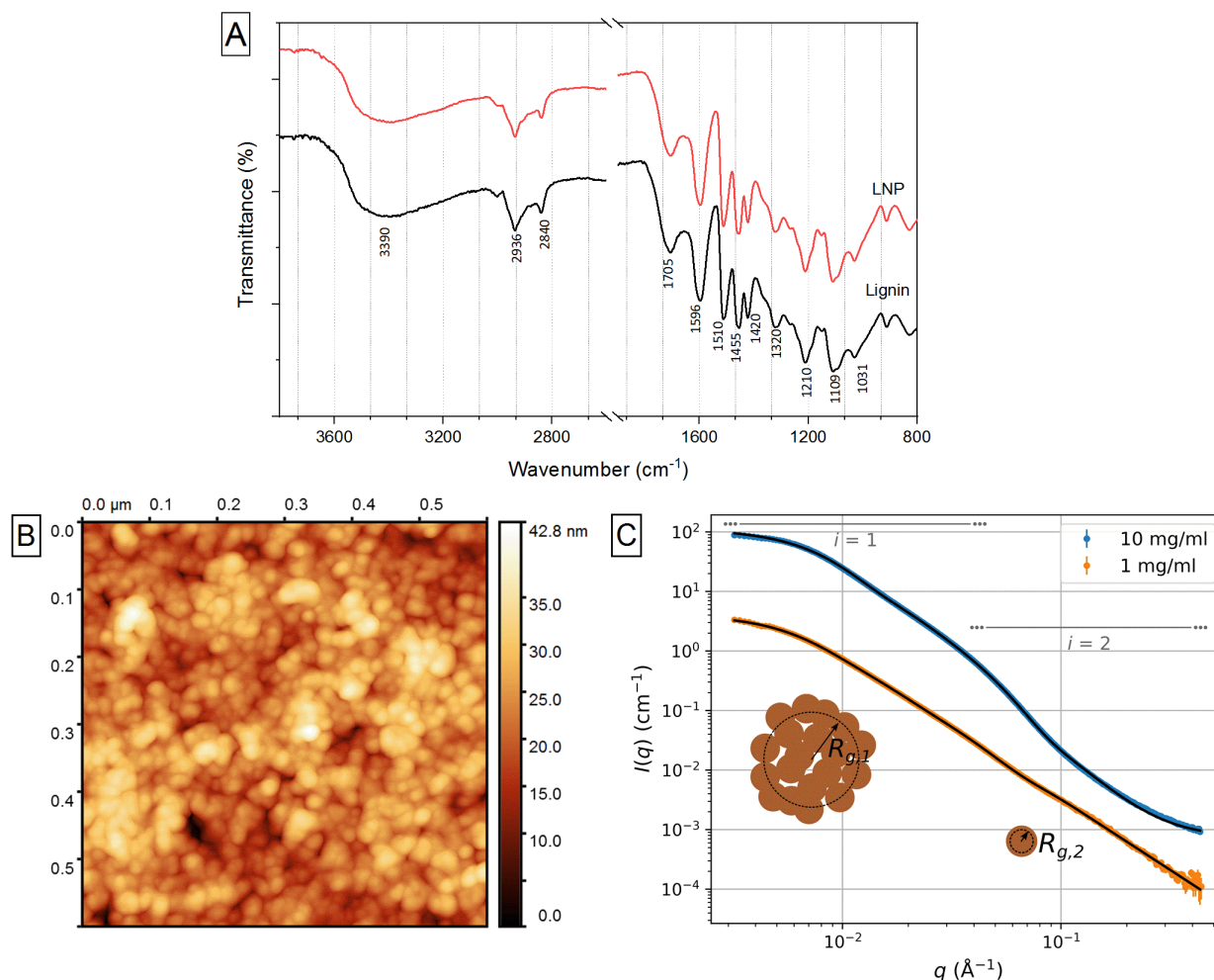


**Figure 2.** Chemical structure, morphology, and nanostructure in aqueous systems of the lignin nanoparticles (LNPs): Fourier-transform infrared spectra in comparison to the original lignin (a), atomic force micrograph of a diluted and air-dried LNP suspension (b), and small-angle x-ray scattering intensities of LNPs in aqueous solution, with fits of the unified exponential/power-law model with two levels of structural hierarchy ( $i=1, 2$ ) drawn with solid lines (c).

## Stability

The stability of the LNPs over time and with changes in the properties of the dispersing medium is an important property that defines the suitable applications of LNPs.

The  $D_H$  of the HCl- and  $\text{HNO}_3$ -precipitated LNPs remained the same during storage for 180 days (Figure 3a) while that precipitated by  $\text{H}_2\text{SO}_4$  showed an increasing trend with time. The highly negative charge on the surface of the particles probably prevented agglomeration, leading to a stable LNP suspension. The particle size of the isolated LNPs was pH-dependent (Figure 3b). Agglomeration occurred at pH 2 resulting in the sedimentation of particles, which is not suitable for DLS measurement. The  $D_H$  increased but the distribution was still monomodal at pH 3.3. The increase in  $D_H$  at pH 3.3 could be attributed to agglomeration induced by intermolecular hydrogen bonding between particles when the carboxyl groups were protonated,<sup>34</sup> which also led to the decrease in

1  
2  
3  
4 368  $\zeta$ -potential (-30 mV). At pH 4.1–7.1, the LNPs remained stable and showed similar size  
5  
6  
7 369 distribution. The  $D_H$  again increased at pH 8.8, even without a significant change in  $\zeta$ -  
8  
9  
10 370 potential. This increase in particle size at alkaline pH can be ascribed to polyelectrolyte  
11  
12  
13  
14 371 swelling, due to breaking of intramolecular hydrogen bonds and dissociation of ionizable  
15  
16  
17 372 functional groups.<sup>35</sup> At pH higher than 10, dissolution occurred, as indicated by the  
18  
19  
20  
21 373 darkening of the suspension. The isolated LNPs appeared stable at a pH range of 4–7.

22  
23  
24 374 The LNPs were also highly affected by the change in ionic strength of the dispersing  
25  
26  
27  
28 375 medium (Figure 3c). At NaCl concentrations up to 0.1 M, the size distribution remained  
29  
30  
31 376 the same. However, at 0.25 M NaCl and higher, agglomeration occurred and the  $\zeta$ -  
32  
33  
34  
35 377 potential also decreased to -10 mV. The increase in ionic strength possibly compressed  
36  
37  
38 378 the electric double-layer and decreased the repulsive forces between particles, leading  
39  
40  
41  
42 379 to agglomeration.<sup>44</sup> These types of LNP, whose stability is dependent on pH or ionic  
43  
44  
45 380 strength, have found applications in controlled drug delivery systems that release drugs  
46  
47  
48  
49 381 upon changes in pH or ionic strength of the surrounding medium.<sup>11</sup>

50  
51  
52 382  
53  
54  
55  
56  
57  
58  
59  
60

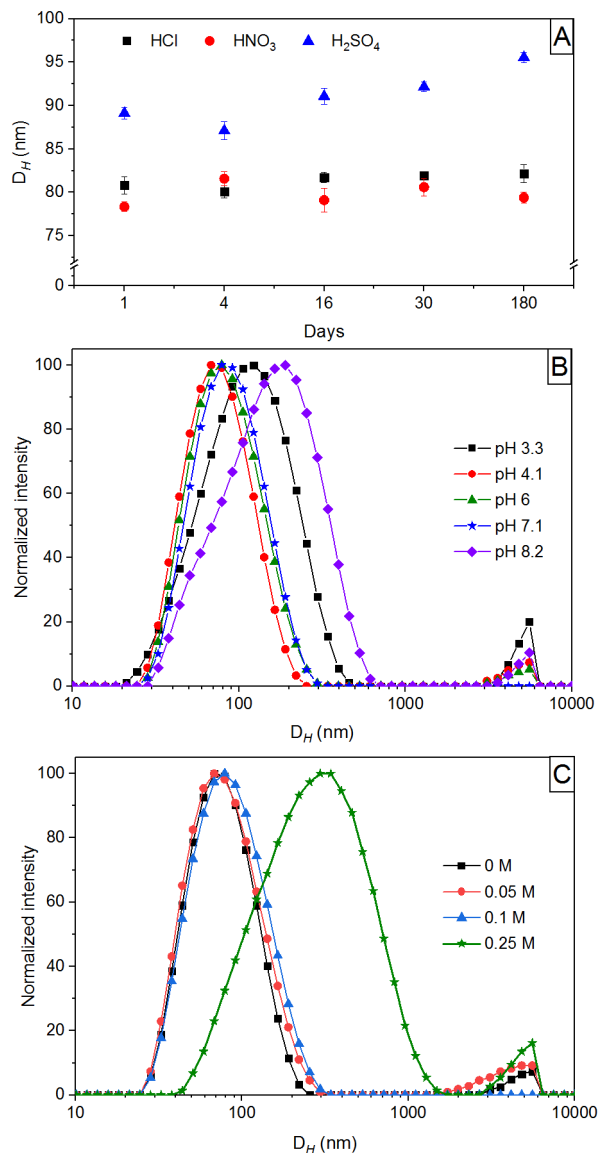


**Figure 3.** Stability of the lignin nanoparticles monitored by the changes in the average hydrodynamic diameter,  $D_H$ , as affected by different factors: storage time (a), variation in pH (b), and salt concentration (c) of the dispersing medium.

## 390 Optimization

391 Optimization of the method was carried out to investigate the effects of different  
392 preparation conditions on the properties of LNPs. Among  $\text{HNO}_3$  and  $\text{HCl}$ , both of which  
393 yielded similar sizes of LNPs,  $\text{HCl}$  was chosen for further optimization because it provided  
394 the highest yield of LNPs among the acids.

395 The  $D_H$  increased with the molar concentration of  $\text{HCl}$ , but still remained within the  
396 nanoscale range (Figure 4a). Diluting the lignin concentration in the APL, with 0.25 M  $\text{HCl}$   
397 used for precipitation, decreased the  $D_H$  (Figure 4b). A similar observation was also  
398 reported previously<sup>16</sup> in the self-assembly formation of LNPs in THF by dialysis against  
399 water. There, a higher initial lignin concentration allowed a greater amount of lignin to  
400 participate in the growth of nanoparticles via the nucleation mechanism. Also in our case,  
401 the formation of large aggregates during precipitation was favored when the final  
402 concentration of lignin, relative to the combined volume of the alkaline liquor and acid  
403 solution, increased. These large lignin aggregates, when subjected to similar ultrasonic  
404 conditions, eventually produced large LNPs. Interestingly, for LNPs obtained directly from

the APL without dilution, i.e. with 20 wt% lignin, an increase in sonication time to 7.5 min already yielded  $D_H$  of less than 100 nm. Thus, with proper optimization of the sonication parameters, LNPs can be prepared directly from the APL, enabling LNP suspensions with much higher concentrations than those reported from previous studies<sup>14,16,23–25</sup>.

Sequential pH precipitation was performed to fractionate the LNPs at pH 6, 4, and 2 to identify the optimum pH for precipitation. The fractional yields at pH 6, 4, and 2 were 3%, 95%, and 2%, respectively. Moreover, only the fraction at pH 4 showed particles in the nanoscale range (Figure 4c). The pH 6 fraction showed the largest particle size, possibly because as the acid was added, large particles precipitated first. The pH 2 fraction also yielded lignin particles with  $D_H$  of more than 100 nm and with the lowest  $\zeta$ -potential (-43 mV), which must have induced agglomeration.

The findings that most of the lignin in the APL can be precipitated at pH 4 highlighted the potential for reducing acid consumption and shortening the dialysis time. Thus, further optimization was carried out to make the process easy to upscale in industry. First, direct pH 4 precipitation, with lower amounts of acid and shorter dialysis times than direct pH 2 precipitation, was performed. Results showed that the size distribution was unimodal and

the average  $D_H$  was 75 ( $\pm$  3) nm, similar to those from direct pH 2 precipitation. To determine if we could completely eliminate dialysis, the suspension from direct pH 4 precipitation was sonicated after decanting the acidic supernatant from centrifugation. The particles from three separate trials were larger and less stable than those obtained with dialysis. The results within the replicated trials were also not reproducible, having in one instance monodispersed LNPs with  $D_H$  less than 100 nm. These irreproducible results could be attributed to the difficulty in removing to the same extent the residual salts and acids only by centrifugation and decantation. These residual salts and acids could have altered the ionic strength and pH of the LNP suspension, whose stability was affected by changes in the ionic strength and pH of the dispersing medium. Nevertheless, the optimization revealed that sufficient removal of residual salts and acids by centrifugation and decantation, which probably occurred in one of the trials, would enable also other options than dialysis. Other methods, such as ultrafiltration, could be more feasible on an industrial scale than dialysis.



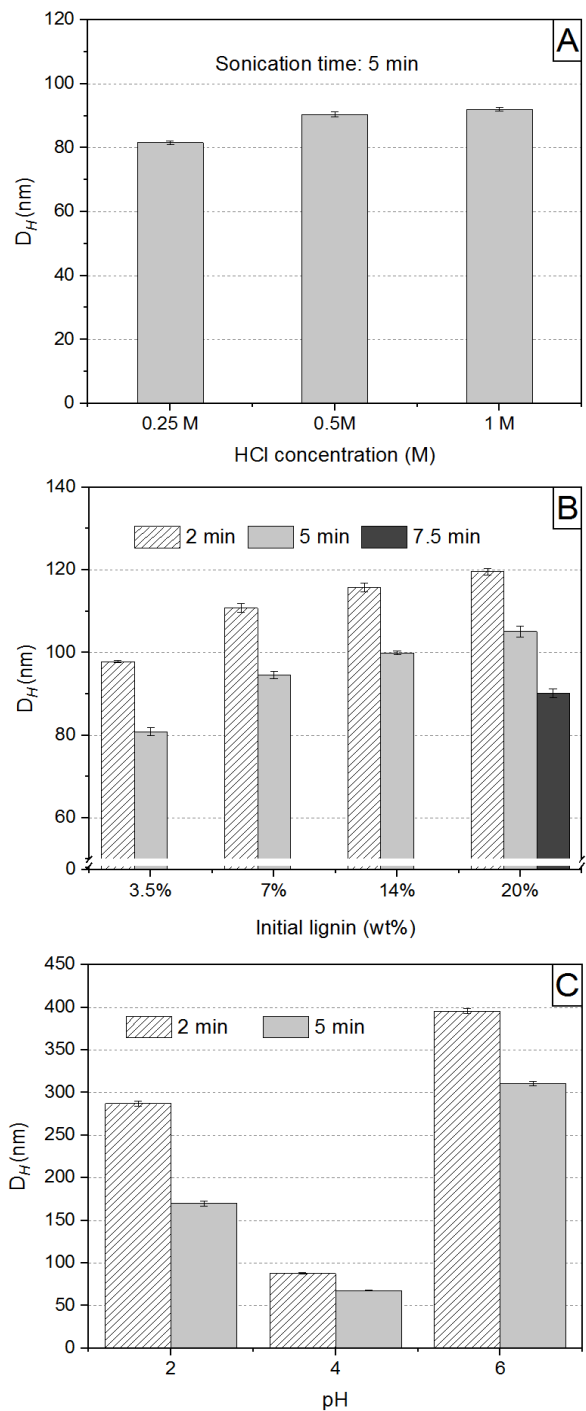


**Figure 4.** Average hydrodynamic diameter ( $D_H$ ) of lignin nanoparticles produced by combined acid precipitation and ultrasonication, as affected by different optimization

parameters: concentration of hydrochloric acid (HCl) (a), initial lignin concentration (b), and sequential pH precipitation (c). The error bars represent  $\pm$  standard deviations of at least three measurements.

#### Comparison with dried lignin

The results clearly indicate the relative ease in producing LNPs directly from the APL without the use of organic solvents or extensive mechanical disintegration procedures.

The mild ultrasonication was achieved by eliminating the drying step, which potentially rendered lignin resistant to mechanical disintegration. To further demonstrate the effect of drying, we dried and sonicated the same acid-precipitated lignin, following the sonication conditions we used with the never-dried lignin. Even at a concentration of only 2 wt%, no LNPs were formed after 90 min of sonication. The particles showed a bimodal distribution with two peaks of approx. 200 and 600 nm (Figure S5). Clearly, drying induced chemical, physical, or structural changes in the lignin, making it more difficult to disintegrate into nanoparticles. Possibly, in the wet state after acid precipitation and dialysis, the agglomerated lignin, apart from lignin-lignin interactions (H-bonding, Van der

1  
2  
3  
4 455 Waals,  $\pi$ - $\pi$ ),<sup>36</sup> maintains its interaction with water. This interaction with water may have  
5  
6  
7 456 resulted in the trapping of water molecules within the aggregates, forming swollen  
8  
9  
10 457 precipitates. During drying, the lignin-water interaction, as we would expect, is removed  
11  
12  
13  
14 458 as the water molecules evaporate. The removal of water possibly caused the lignin  
15  
16  
17 459 aggregates to collapse and form rigid, compact lignin particles, which are more difficult to  
18  
19  
20  
21 460 disintegrate than a swollen precipitate.  
22  
23

24 461 This concept of producing nanomaterials by mechanical disintegration from a never-  
25  
26  
27  
28 462 dried bio-based material has also been demonstrated in the preparation of nanofibrillated  
29  
30  
31 463 cellulose.<sup>37,38</sup> The reason was the phenomenon called 'hornification', which is the  
32  
33  
34  
35 464 irreversible aggregation of cellulose microfibrils brought about by the formation of H-  
36  
37  
38 465 bonds, creating fixed domains that are not easily accessible by water.<sup>39</sup> Although the  
39  
40  
41  
42 466 effect of drying on the properties of lignin is not as well studied as in cellulose, we  
43  
44  
45 467 demonstrated that the preparation of LNPs is easily achieved from a lignin that was not  
46  
47  
48  
49 468 dried before ultrasonication.  
50  
51

52 469 This simple method, without using hazardous organic solvents and in a relatively short  
53  
54  
55  
56 470 period, already achieved LNP suspensions with an average concentration of 3 wt%.  
57  
58  
59  
60

Concentrations higher than 3 wt% were even achievable if precipitating directly from the APL and with a slight increase in sonication time to 7.5 min. Previous reports of LNP preparation, apart from using toxic organic solvents, mostly used relatively low concentrations of lignin (often < 1 wt%).<sup>11</sup> Aqueous acid precipitation, which yielded LNPs with an average size of 89 nm, was also reported,<sup>14</sup> but the initial concentration of lignin in the alkaline solution was only 0.05 wt%. Direct ultrasonication<sup>23,24</sup> of aqueous lignin dispersions prepared from dry lignin also produced LNPs but the sonication times were 1 h and 6 h for 0.7 wt% and 1 wt% lignin, respectively. High-shear homogenization of a 5 g L<sup>-1</sup>(~0.5 wt%) aqueous dispersion of an acid-precipitated lignin after freeze-drying required 4 h to produce LNPs. In our case, a very mild ultrasonication procedure was sufficient to disintegrate the never-dried lignin precipitate.

## Emulsifying properties

Inherent in the amphiphilic characteristic of lignin, the isolated LNPs showed excellent emulsifying properties. As shown in Figure 5, oil-in-water emulsions with varying amounts of LNPs as emulsifying agents can be produced without additional surfactant. The droplet

size also decreased and became uniform as the LNP content increased. At 0.60 wt% LNP, droplet sizes of about 1  $\mu\text{m}$ , based on DLS, were produced.

The stability of the emulsion over 21 days was also assessed using a turbiscan meter.

The backscattered and transmitted lights, which were detected at  $45^\circ$  and  $180^\circ$ , respectively, from the incident light, were used to derive a parameter called the turbiscan stability index (TSI). The higher the value of the TSI, the less stable the emulsion. As seen in Figure 5e, the stability of the emulsion increased with increasing concentrations of lignin, and the trend was prominent during the first week after emulsion preparation. Later, the TSI values of the emulsion with 0.15% LNP plateaued, which does not indicate stability but merely the absence of changes in scattered and transmitted radiations due to creaming. As seen in the profile of the backscattering intensity (Figure 5f), creaming already occurred in the emulsion with 0.15% LNP on day 3. This finding highlights the potential use of the isolated LNPs without additional chemical modification as stabilizers of interfaces in multiphase systems for various applications.

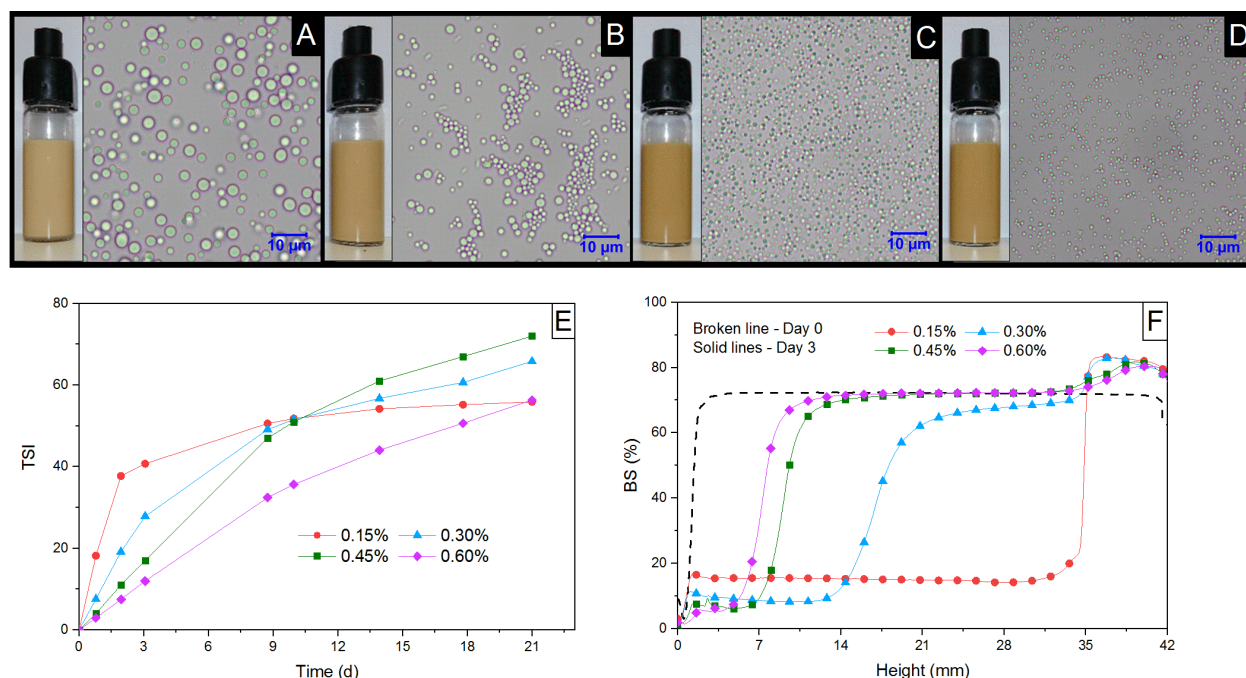


**Figure 5.** Oil-in-water emulsions with varying amounts of hydrochloric acid-precipitated lignin nanoparticles : (a) 0.15, (b) 0.30, (c) 0.45, and (d) 0.60 wt% with the corresponding optical images (100x objective lens) and the stability of the emulsions represented by the values of the turbiscan stability index (TSI, e) and backscattering intensity (BS%, f).

## CONCLUSIONS

A simple green method for LNP preparation from APL was demonstrated using a combined acid precipitation and ultrasonication procedure. The mild ultrasonication of only 5 min was done directly without prior drying the acid-precipitated lignin. The method thus eliminates the drying step usually done in industries when recovering the lignin from

the pulp liquor. Eliminating the drying step favorably rendered the acid-precipitated lignin easy to disintegrate by ultrasonication, making the entire process energy-efficient and rapid. The combined method afforded the production of stable, highly charged, spherical LNPs, with hierarchical nanostructure in aqueous systems. Optimization of the method also showed favorable potential for producing LNPs directly from the APL, i.e. without dilution, enabling a concentrated LNP suspension. Furthermore, acid consumption and dialysis time can be minimized by precipitating at pH 4 rather than at pH 2. Sufficient removal of residual salts and acids is needed to obtain stable LNPs and reproducible results. The isolated LNPs without additional surfactant can emulsify oil in water and form stable emulsions for several days. This method, which does not use hazardous organic solvents or intensive ultrasonication, opens a green, sustainable, and highly scalable approach to producing LNPs directly from APL. Finally, the developed method enables the production of solvent-free LNPs, which can be further explored for their potential as bio-based interfacial stabilizers in the food and medical industries.

526

527 ASSOCIATED CONTENT

**Supporting Information.** The following files are available free of charge: FTIR spectra and table summarizing band assignments; 2D-HSQC-NMR spectrum of the isolated LNPs; AFM micrographs; contributions of different terms in the fits of the unified model to the SAXS intensities; fitting results of the unified model to the SAXS intensities; size distribution chromatograms of dried and never-dried lignin after ultrasonication.

## AUTHOR INFORMATION

### Author Contributions

The manuscript was written through contributions of all authors. All authors have given approval to the final version of the manuscript. KSM<sup>†,§</sup> supervised the work, MBA<sup>†</sup> performed all the experiments (except SAXS and HSQC NMR) and wrote the paper, PAP<sup>‡</sup> and ML<sup>†</sup> analyzed, interpreted, and wrote the discussion for the SAXS and HSQC-NMR data, respectively.

### Funding Sources



1  
2  
3  
4  
5  
6  
7  
8  
9  
10  
11  
12  
13  
14  
15  
16  
17  
18  
19  
20  
21  
22  
23  
24  
25  
26  
27  
28  
29  
30  
31  
32  
33  
34  
35  
36  
37  
38  
39  
40  
41  
42  
43  
44  
45  
46  
47  
48  
49  
50  
51  
52  
53  
54  
55  
56  
57  
58  
59  
60

541 Faculty of Agriculture and Forestry, University of Helsinki and Academy of Finland,  
542 grant no. 315768 (P.A.P.)

543 **Notes.** The authors declare no conflict of interests.

544 ACKNOWLEDGMENT

545 We acknowledge Miikka Mattinen for his valuable help with imaging using AFM,  
546 Mamata Bhattarai for her assistance in the DLS experiment, and Julia Varis for drawing  
547 the TOC abstract. We also thank the NMR core facility supported by the University of  
548 Helsinki and Biocenter Finland, the AFM facility at the Department of Chemistry,  
549 University of Helsinki, and CH Bioforce for providing the sample. P.A.P. thanks the  
550 Academy of Finland (grant no. 315768) for funding and Dr. Claire Pizzey from Diamond  
551 Light Source for conducting the SAXS measurements.

553 REFERENCES

554 (1) Xu, Z.; Lei, P.; Zhai, R.; Wen, Z.; Jin, M. Recent Advances in Lignin Valorization  
555 with Bacterial Cultures: Microorganisms, Metabolic Pathways, and Bio-Products.

- 556 *Biotechnol. Biofuels* **2019**, *12* (1), 1–19. [https://doi.org/10.1186/s13068-019-1376-](https://doi.org/10.1186/s13068-019-1376-0)
- 557 0.
- 558 (2) Ragauskas, A. J.; Beckham, G. T.; Biddy, M. J.; Chandra, R.; Chen, F.; Davis, M.
- 559 F.; Davison, B. H.; Dixon, R. A.; Gilna, P.; Keller, M.; et al. Lignin Valorization:
- 560 Improving Lignin Processing in the Biorefinery. *Science* (80-. ). **2014**, *344*
- 561 (1246843). <https://doi.org/10.1126/science.1246843>.
- 562 (3) Bruijninx, P. C. A.; Rinaldi, R.; Weckhuysen, B. M. Unlocking the Potential of a
- 563 Sleeping Giant: Lignins as Sustainable Raw Materials for Renewable Fuels,
- 564 Chemicals and Materials. *Green Chem.* **2015**, *17* (11), 4860–4861.
- 565 <https://doi.org/10.1039/c5gc90055g>.
- 566 (4) Nagy, M.; Kosa, M.; Theliander, H.; Ragauskas, A. J. Characterization of CO<sub>2</sub>
- 567 Precipitated Kraft Lignin to Promote Its Utilization. *Green Chem.* **2010**, *12* (1), 31–
- 568 34. <https://doi.org/10.1039/b913602a>.
- 569 (5) Langholtz, M.; Downing, M.; Graham, R.; Baker, F.; Compere, A.; Griffith, W.;
- 570 Boeman, R.; Keller, M. Lignin-Derived Carbon Fiber as a Co-Product of Refining

- 571 Cellulosic Biomass. *SAE Int. J. Mater. Manuf.* **2014**, *7*(1), 115–121.
- 572 (6) Collins, M. N.; Nechifor, M.; Tanasă, F.; Zănoagă, M.; McLoughlin, A.; Stróżyk, M.  
573 A.; Culebras, M.; Teacă, C. A. Valorization of Lignin in Polymer and Composite  
574 Systems for Advanced Engineering Applications – A Review. *Int. J. Biol. Macromol.*  
575 **2019**, *131*, 828–849. <https://doi.org/10.1016/j.ijbiomac.2019.03.069>.
- 576 (7) Sipponen, M. H.; Lange, H.; Crestini, C.; Henn, A.; Österberg, M. Lignin for Nano-  
577 and Microscaled Carrier Systems: Applications, Trends and Challenges. *ChemSusChem*  
578 **2019**, *12*(10), 2039–2054. <https://doi.org/DOI:10.1002/cssc.201900480>.
- 579 (8) Beisl, S.; Friedl, A.; Miltner, A. Lignin from Micro- to Nanosize: Applications. *Int. J.*  
580 *Mol. Sci.* **2017**, *18*(11), 2367. <https://doi.org/10.3390/ijms18112367>.
- 581 (9) Kai, D.; Tan, M. J.; Chee, P. L.; Chua, Y. K.; Yap, Y. L.; Loh, X. J. Towards Lignin-  
582 Based Functional Materials in a Sustainable World. *Green Chem.* **2016**, *18*(5),  
583 1175–1200. <https://doi.org/10.1039/c5gc02616d>.
- 584 (10) Figueiredo, P.; Lintinen, K.; Hirvonen, J. T.; Kostianen, M. A.; Santos, H. A.

- 585 Properties and Chemical Modifications of Lignin: Towards Lignin-Based  
586 Nanomaterials for Biomedical Applications. *Prog. Mater. Sci.* **2018**, *93*, 233–269.  
587 <https://doi.org/10.1016/j.pmatsci.2017.12.001>.
- (11) Beisl, S.; Friedl, A.; Miltner, A. Lignin from Micro- To Nanosize: Production  
588 Methods. *Int. J. Mol. Sci.* **2017**, *18* (11), 1244.  
589 <https://doi.org/10.3390/ijms18112367>.
- (12) Bangalore Ashok, R. P.; Oinas, P.; Lintinen, K.; Sarwar, G.; Kostianen, M. A.;  
592 Österberg, M. Techno-Economic Assessment for the Large-Scale Production of  
593 Colloidal Lignin Particles. *Green Chem.* **2018**, *20* (21), 4911–4919.  
594 <https://doi.org/10.1039/c8gc02805b>.
- (13) Abbati De Assis, C.; Greca, L. G.; Ago, M.; Balakshin, M. Y.; Jameel, H.; Gonzalez,  
595 R.; Rojas, O. J. Techno-Economic Assessment, Scalability, and Applications of  
596 Aerosol Lignin Micro- and Nanoparticles. *ACS Sustain. Chem. Eng.* **2018**, *6* (9),  
597 11853–11868. <https://doi.org/10.1021/acssuschemeng.8b02151>.
- (14) Frangville, C.; Rutkevičius, M.; Richter, A. P.; Velez, O. D.; Stoyanov, S. D.;

- 600 Paunov, V. N. Fabrication of Environmentally Biodegradable Lignin Nanoparticles.
- 601 *ChemPhysChem* **2012**, *13* (18), 4235–4243.
- 602 <https://doi.org/10.1002/cphc.201200537>.
- 603 (15) Yang, W.; Fortunati, E.; Gao, D.; Balestra, G. M.; Giovanale, G.; He, X.; Torre, L.;
- 604 Kenny, J. M.; Puglia, D. Valorization of Acid Isolated High Yield Lignin
- 605 Nanoparticles as Innovative Antioxidant/Antimicrobial Organic Materials. *ACS*
- 606 *Sustain. Chem. Eng.* **2018**, *6* (3), 3502–3514.
- 607 <https://doi.org/10.1021/acssuschemeng.7b03782>.
- 608 (16) Lievonen, M.; Valle-Delgado, J. J.; Mattinen, M. L.; Hult, E. L.; Lintinen, K.;
- 609 Kostianen, M. A.; Paananen, A.; Szilvay, G. R.; Setälä, H.; Österberg, M. A Simple
- 610 Process for Lignin Nanoparticle Preparation. *Green Chem.* **2016**, *18* (5), 1416–
- 611 1422. <https://doi.org/10.1039/c5gc01436k>.
- 612 (17) Qian, Y.; Deng, Y.; Qiu, X.; Li, H.; Yang, D. Formation of Uniform Colloidal Spheres
- 613 from Lignin, a Renewable Resource Recovered from Pulp Spent Liquor. *Green*
- 614 *Chem.* **2014**, *16* (4), 2156–2163. <https://doi.org/10.1039/c3gc42131g>.

- 615 (18) Li, H.; Deng, Y.; Liang, J.; Dai, Y.; Liu, B.; Ren, Y.; Qiu, X.; Li, C. Direct Preparation  
616 of Hollow Nanospheres with Kraft Lignin: A Facile Strategy for Effective Utilization  
617 of Biomass Waste. *BioResources* **2016**, *11* (2), 3073–3083.  
618 <https://doi.org/10.15376/biores.11.2.3073-3083>.
- 619 (19) Tian, D.; Hu, J.; Bao, J.; Chandra, R. P.; Saddler, J. N.; Lu, C. Lignin Valorization:  
620 Lignin Nanoparticles as High-Value Bio-Additive for Multifunctional  
621 Nanocomposites. *Biotechnol. Biofuels* **2017**, *10* (1), 1–11.  
622 <https://doi.org/10.1186/s13068-017-0876-z>.
- 623 (20) Li, H.; Deng, Y.; Wu, H.; Ren, Y.; Qiu, X.; Zheng, D.; Li, C. Self-Assembly of Kraft  
624 Lignin into Nanospheres in Dioxane-Water Mixtures. *Holzforschung* **2016**, *70* (8),  
625 725–731. <https://doi.org/10.1515/hf-2015-0238>.
- 626 (21) Nair, S. S.; Sharma, S.; Pu, Y.; Sun, Q.; Pan, S.; Zhu, J. Y.; Deng, Y.; Ragauskas,  
627 A. J. High Shear Homogenization of Lignin to Nanolignin and Thermal Stability of  
628 Nanolignin-Polyvinyl Alcohol Blends. *ChemSusChem* **2014**, *7* (12), 3513–3520.  
629 <https://doi.org/10.1002/cssc.201402314>.

- 630 (22) Matsakas, L.; Karnaouri, A.; Cwirzen, A.; Rova, U.; Christakopoulos, P. Formation  
631 of Lignin Nanoparticles by Combining Organosolv Pretreatment of Birch Biomass  
632 and Homogenization Processes. *Molecules* **2018**, *23* (7), 1822.  
633 <https://doi.org/10.3390/molecules23071822>.
- 634 (23) Gilca, I. A.; Popa, V. I.; Crestini, C. Obtaining Lignin Nanoparticles by Sonication.  
635 *Ultrason. Sonochem.* **2015**, *23*, 369–375.  
636 <https://doi.org/10.1016/j.ultsonch.2014.08.021>.
- 637 (24) Garcia Gonzalez, M. N.; Levi, M.; Turri, S.; Griffini, G.; Gonzalez Garcia, M. N.;  
638 Levi, M.; Turri, S.; Griffini, G. Lignin Nanoparticles by Ultrasonication and Their  
639 Incorporation in Waterborne Polymer Nanocomposites. *J. Appl. Polym. Sci.* **2017**,  
640 *134* (38), 1–10. <https://doi.org/10.1002/app.45318>.
- 641 (25) Yin, H.; Liu, L.; Wang, X.; Wang, T.; Zhou, Y.; Liu, B.; Shan, Y.; Wang, L.; Lü, X. A  
642 Novel Flocculant Prepared by Lignin Nanoparticles-Gelatin Complex from  
643 Switchgrass for the Capture of Staphylococcus Aureus and Escherichia Coli.  
644 *Colloids Surfaces A Physicochem. Eng. Asp.* **2018**, *545* (December 2017), 51–59.

645 <https://doi.org/10.1016/j.colsurfa.2018.02.033>.

646 (26) Peters, D. Ultrasound in Materials Chemistry. *J. Mater. Chem.* **1996**, *6* (10), 1605–  
647 1618.

648 (27) Tortora, M.; Cavalieri, F.; Mosesso, P.; Ciaffardini, F.; Melone, F.; Crestini, C.  
649 Ultrasound Driven Assembly of Lignin into Microcapsules for Storage and Delivery  
650 of Hydrophobic Molecules. *Biomacromolecules* **2014**, *15* (5), 1634–1643.  
651 <https://doi.org/10.1021/bm500015j>.

652 (28) von Schoultz, S. Method for Extracting Lignin. WO 2015104460, 2016.

653 (29) Lagerquist, L.; Pranovich, A.; Smeds, A.; von Schoultz, S.; Vähäsalo, L.; Rahkila,  
654 J.; Kilpeläinen, I.; Tamminen, T.; Willför, S.; Eklund, P. Structural Characterization  
655 of Birch Lignin Isolated from a Pressurized Hot Water Extraction and Mild Alkali  
656 Pulped Biorefinery Process. *Ind. Crops Prod.* **2018**, *111*, 306–316.  
657 <https://doi.org/10.1016/j.indcrop.2017.10.040>.

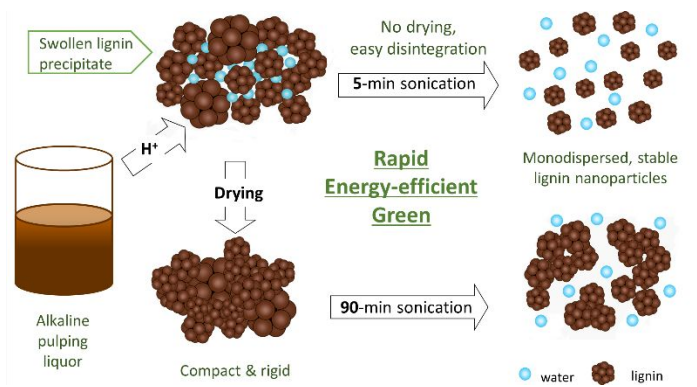
658 (30) Beaucage, G. Approximations Leading to a Unified Exponential/Power-Law



- 659 Approach to Small-Angle Scattering. *J. Appl. Crystallogr.* **1995**, *28* (6), 717–728.
- 660 <https://doi.org/10.1107/S0021889895005292>.
- 661 (31) Doucet, M.; Hie, J.; Gervaise, A.; Bouwman, W.; Campbell, K.; Gonzales, M.;
- 662 Heenan, R.; King, S.; Kienzle, P.; Jackson, A.; et al. *SasView Version 4.2*, 2019.
- 663 <https://doi.org/http://doi.org/10.5281/zenodo.1412041>.
- 664 (32) Vainio, U.; Maximova, N.; Hortling, B.; Laine, J.; Stenius, P.; Simola, L. K.; Gravitis,
- 665 J.; Serimaa, R. Morphology of Dry Lignins and Size and Shape of Dissolved Kraft
- 666 Lignin Particles by X-Ray Scattering. *Langmuir* **2004**, *20* (22), 9736–9744.
- 667 <https://doi.org/10.1021/la048407v>.
- 668 (33) Salentinig, S.; Schubert, M. Softwood Lignin Self-Assembly for Nanomaterial
- 669 Design. *Biomacromolecules* **2017**, *18* (8), 2649–2653.
- 670 <https://doi.org/10.1021/acs.biomac.7b00822>.
- 671 (34) Lindström, T. The Colloidal Behaviour of Kraft Lignin and Lignosulfonates. *Colloid*
- 672 *Polym. Sci.* **1980**, *258*, 168–173. [https://doi.org/10.1016/0166-6622\(86\)80087-7](https://doi.org/10.1016/0166-6622(86)80087-7).

- (35) Garver, T. M.; Callaghan, P. T. Hydrodynamics of Kraft Lignins. *Macromolecules* **1991**, *24* (2), 420–430. <https://doi.org/10.1021/ma00002a013>.
- (36) Zhao, W.; Xiao, L. P.; Song, G.; Sun, R. C.; He, L.; Singh, S.; Simmons, B. A.; Cheng, G. From Lignin Subunits to Aggregates: Insights into Lignin Solubilization. *Green Chem.* **2017**, *19* (14), 3272–3281. <https://doi.org/10.1039/c7gc00944e>.
- (37) Abe, K.; Iwamoto, S.; Yano, H. Obtaining Cellulose Nanofibers with a Uniform Width of 15nm from Wood. *Biomacromolecules* **2007**, *8*, 3276–3278.
- (38) Iwamoto, S.; Nakagaito, A. N.; Yano, H. Nano-Fibrillation of Pulp Fibers for the Processing of Transparent Nanocomposites. *Appl. Phys. A* **2007**, *89* (2), 461–466. <https://doi.org/10.1007/s00339-007-4175-6>.
- (39) Röder, T.; Sixta, H. Thermal Treatment of Cellulose Pulps and Its Influence to Cellulose Reactivity. *Lenzinger Berichte* **2004**, *83*, 79–83.

TOC Abstract



Synopsis: A facile, rapid and energy-efficient route of preparing lignin nanoparticles directly from alkaline pulping liquor was developed.

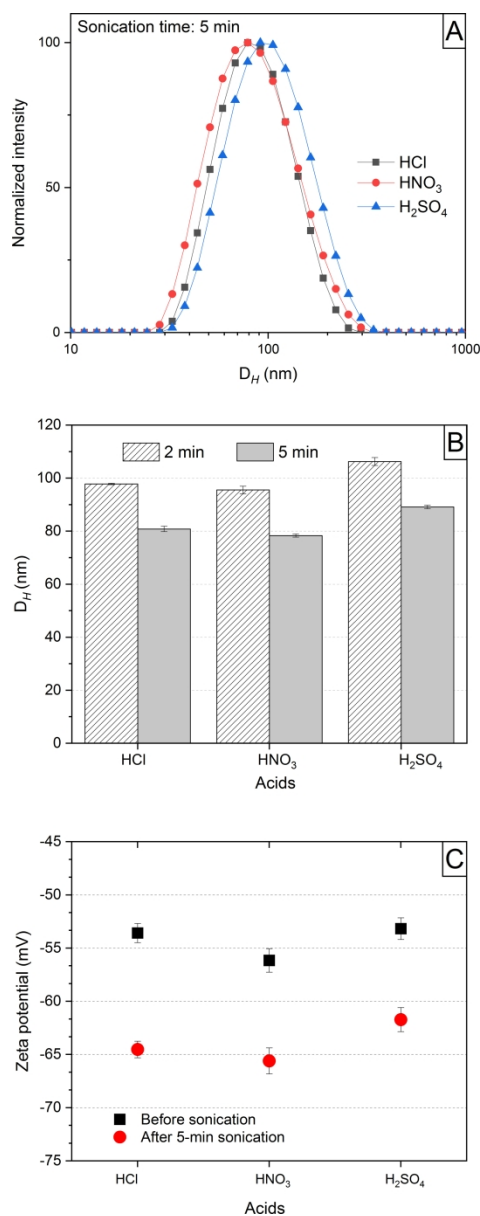


Figure 1. Effect of acid type on the intensity-based hydrodynamic diameter (DH) distribution (a), average DH (b), and average zeta potential (c) of lignin nanoparticles prepared from alkaline pulping liquor by the combined acid precipitation and ultrasonication method. The error bars represent  $\pm$  standard deviations of at least three measurements.

84x215mm (600 x 600 DPI)

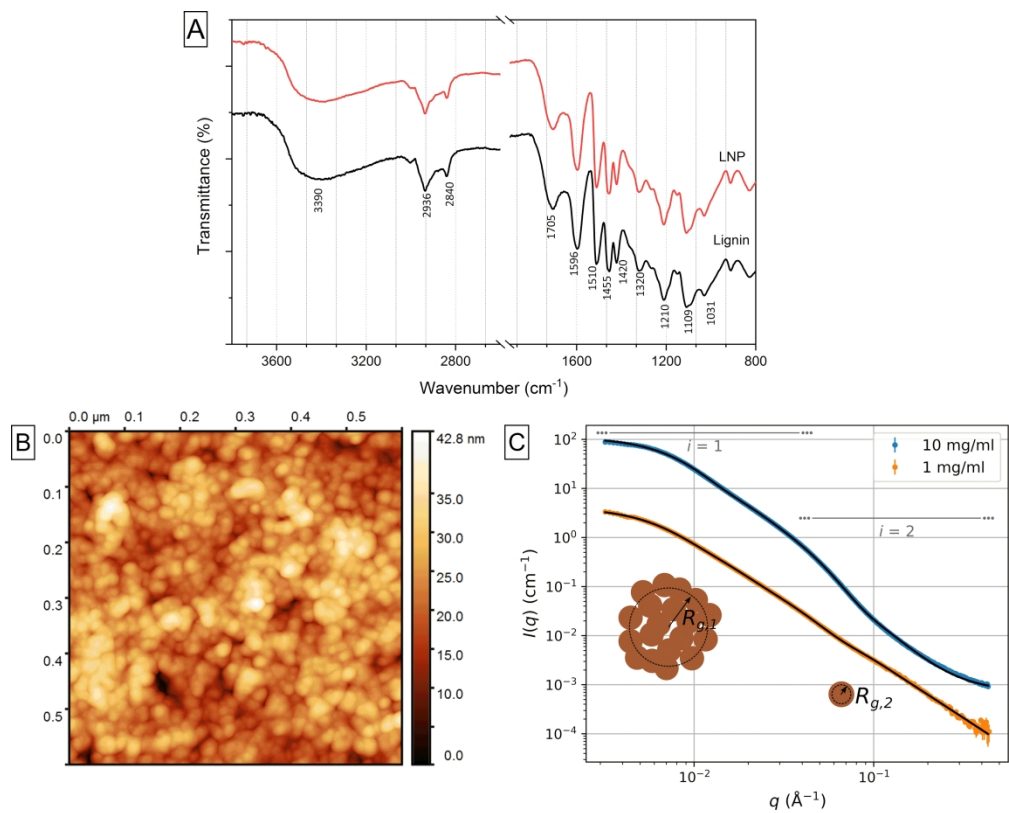


Figure 2. Chemical structure, morphology, and nanostructure in aqueous systems of the lignin nanoparticles (LNPs): Fourier-transform infrared spectra in comparison to the original lignin (a), atomic force micrograph of a diluted and air-dried LNP suspension (b), and small-angle x-ray scattering intensities of LNPs in aqueous solution, with fits of the unified exponential/power-law model with two levels of structural hierarchy ( $i = 1, 2$ ) drawn with solid lines (c).

177x141mm (600 x 600 DPI)

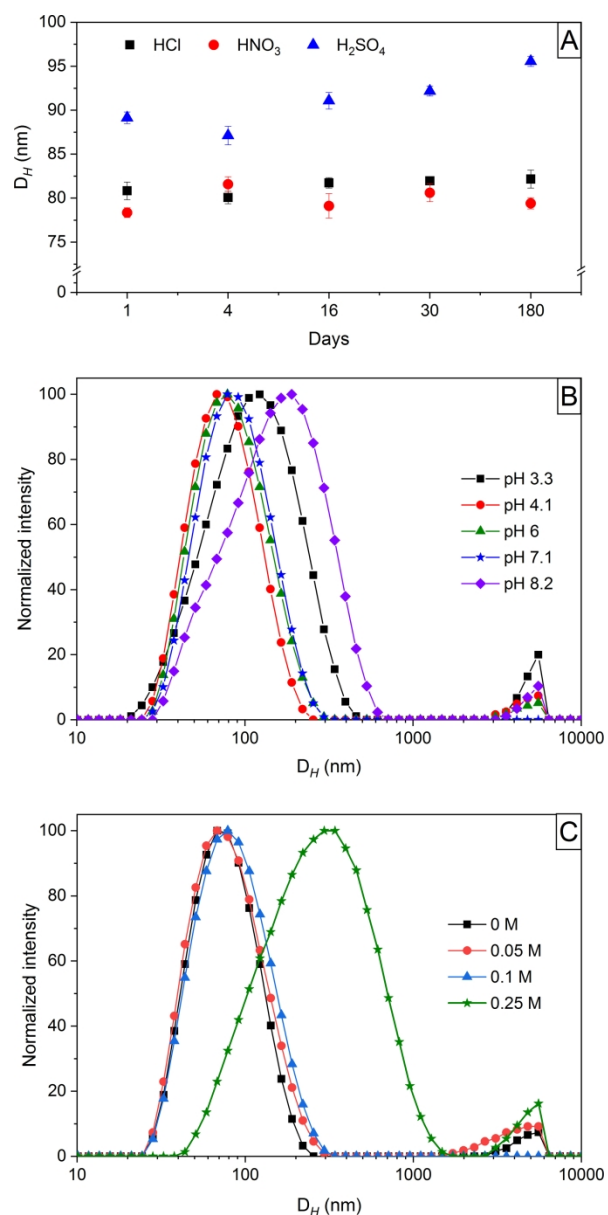


Figure 3. Stability of the lignin nanoparticles monitored by the changes in the average hydrodynamic diameter,  $D_H$ , as affected by different factors: storage time (a), variation in pH (b), and salt concentration (c) of the dispersing medium.

84x171mm (600 x 600 DPI)

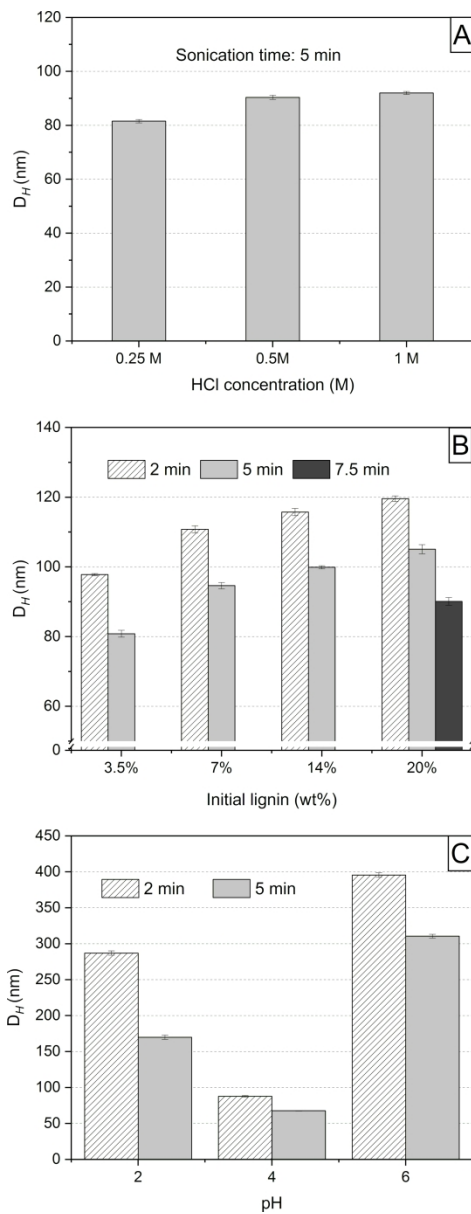


Figure 4. Average hydrodynamic diameter ( $D_H$ ) of lignin nanoparticles produced by combined acid precipitation and ultrasonication, as affected by different optimization parameters: concentration of hydrochloric acid (HCl) (a), initial lignin concentration (b), and sequential pH precipitation (c). The error bars represent  $\pm$  standard deviations of at least three measurements.

84x216mm (600 x 600 DPI)

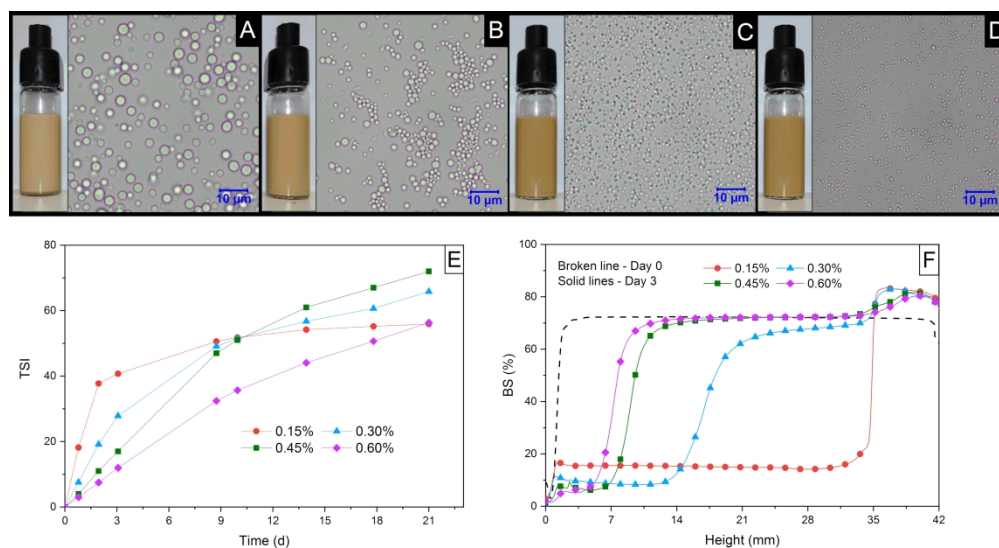


Figure 5. Oil-in-water emulsions with varying amounts of hydrochloric acid-precipitated lignin nanoparticles : 0.15 (a), 0.30 (b), 0.45 (c), and 0.60 (d) wt% with the corresponding optical images (100x objective lens) and the stability of the emulsions represented by the values of the turbiscan stability index (TSI, e) and backscattering intensity (BS%, f).

177x95mm (600 x 600 DPI)